**The EMBO Journal (2012) 31,** 3745–3756 | © 2012 European Molecular Biology Organization | All Rights Reserved 0261-4189/12
www.embojournal.org

THE EMBO JOURNAL

# DEAD-box protein DDX3 associates with eIF4F to promote translation of selected mRNAs

**Ricardo Soto-Rifo[1,2], Paulina S Rubilar[1,2], Taran Limousin[1,2], Sylvain de Breyne[1,2], Didier Décimo[1,2] and Théophile Ohlmann[1,2,3,*]**

[1]Human Virology Department, INSERM U758, Lyon, France, [2]Ecole Normale Supérieure de Lyon, Université de Lyon, Lyon, France and [3]Laboratoire de Virologie, Hospices Civils de Lyon, Lyon, France

**Here, we have characterized a step in translation initiation of viral and cellular mRNAs that contain RNA secondary structures immediately at the vicinity of their m$^7$GTP cap. This is mediated by the DEAD-box helicase DDX3 which can directly bind to the 5′ of the target mRNA where it clamps the entry of eIF4F through an eIF4G and Poly A-binding protein cytoplasmic 1 (PABP) double interaction. This could induce limited local strand separation of the secondary structure to allow 43S pre-initiation complex attachment to the 5′ free extremity of the mRNA. We further demonstrate that the requirement for DDX3 is highly specific to some selected transcripts, cannot be replaced or substituted by eIF4A and is only needed in the very early steps of ribosome binding and prior to 43S ribosomal scanning. Altogether, these data define an unprecedented role for a DEAD-box RNA helicase in translation initiation.**
*The EMBO Journal* (2012) **31,** 3745–3756. doi:10.1038/emboj.2012.220; Published online 7 August 2012
*Subject Categories:* RNA; proteins
*Keywords*: DDX3; DEAD-box RNA helicase; eIF4F; HIV; translation initiation

## Introduction

Recruitment of the 43S pre-initiation complex (PIC) at the 5′ end of an mRNA is the rate-limiting step during translation initiation in eukaryotes. During the early events of this process, the recognition of the m$^7$GTP cap moiety by eIF4F allows the recruitment of the 40S small ribosomal subunit (together with several initiation factors and the met-tRNA$_i$) onto the mRNA (Pestova and Kolupaeva, 2002; Jackson *et al*, 2010). The multimeric complex eIF4F is composed of the cap binding protein eIF4E, the DEAD-box RNA helicase eIF4A and the scaffold protein eIF4G (Jackson *et al*, 2010). Upon cap structure recognition, the ATP-dependent RNA helicase activity of eIF4A is thought to be responsible for the unwinding of secondary structures that favour the movement of the 43S PIC along the 5′-UTR during ribosomal scanning (Parsyan *et al*, 2011). Indeed, the requirement of the eIF4A activity is directly correlated to the amount of secondary structures present within the 5′-UTR (Svitkin *et al*, 2001; Pestova and Kolupaeva, 2002). However, several cellular and viral transcripts harbour unusually long 5′-UTRs composed of multiple stem-loop (SL) structures sufficiently stable to resist the unwinding activity of eIF4A (Kozak, 1991; Pickering and Willis, 2005). This may account for the requirement of additional RNA helicases such as Ded1 in yeast or the DEAH-box proteins DHX29 and RNA helicase A (RHA or DHX9) in mammals, which cooperate with eIF4A to enhance the processivity of ribosomal scanning on structured mRNAs (Parsyan *et al*, 2011). While Ded1 and RHA act by unwinding secondary structures present within the 5′-UTR (Berthelot *et al*, 2004; Hartman *et al*, 2006; Marsden *et al*, 2006), DHX29 has the unique ability to remodel the 40S ribosomal subunit to assist its scanning over RNA structures (Pisareva *et al*, 2008; Parsyan *et al*, 2009; Abaeva *et al*, 2011).

In contrast to RHA, which is recruited by binding to a specific post-transcriptional control element (PCE) present in its selected mRNA targets (Hartman *et al*, 2006), other RNA helicases are delivered to the 5′ end of the mRNA indirectly as a component of eIF4F (eIF4A and Ded1) or together with the 40S ribosomal subunit (DHX29) (Imataka and Sonenberg, 1997; Pisareva *et al*, 2008; Hilliker *et al*, 2011). Indeed, the affinity of eIF4A for RNA is very low and its ATPase and helicase activities are strongly stimulated when present in the eIF4F complex or when it is associated with its co-factors eIF4B and eIF4H (Lorsch and Herschlag, 1998a, b; Rajagopal *et al*, 2012). This indicates that the helicase activity of eIF4A needs to be delivered to the 5′ end of the mRNA by eIF4E/eIF4G upon cap recognition. Consistent with this idea, RNA structures located close to the 5′ end such as the *trans*-activation response element (TAR) present in the transcripts of the human and simian immunodeficiency viruses impair translation by interfering with cap recognition and thus, the recruitment of the eIF4A helicase activity (Parkin *et al*, 1988; Kozak, 1989; Sagliocco *et al*, 1993; Pestova and Kolupaeva, 2002; Babendure *et al*, 2006).

By studying the mechanism of translation initiation of the human immunodeficiency virus type-1 (HIV-1) genomic RNA (gRNA), we came across a molecular mechanism of viral and cellular translational control mediated by the DEAD-box RNA helicase DDX3, a host factor essential for HIV-1 replication (Bushman *et al*, 2009). Although the precise role of DDX3 in translational control remains ambiguous, it was proposed either to assist translation of mRNAs carrying complex 5′-UTRs in an ATP-dependent manner by an unknown mechanism or to promote ribosomal subunit joining in an ATP-independent manner (Lai *et al*, 2008, 2010; Geissler *et al*, 2012). In this manuscript, we have further investigated the ATP-dependent role of DDX3 in viral and cellular translation and we have characterized a molecular mechanism for initial 43S ribosomal binding.

*Corresponding author. Ecole Normale Supérieure de Lyon, INSERM U758 ENS-Lyon, Laboratoire de Virologie, Université de Lyon, Lyon, 69364 France. Tel.: +33 472 728 953; Fax: +33 472 72 81 37; E-mail: tohlmann@ens-lyon.fr

**Received: 19 April 2012; accepted: 11 July 2012; published online: 7 August 2012**

We show that DDX3 is not essential for general translation but is required for translation driven by cellular and viral transcripts that contain secondary structures within their 5′-UTR. By using the HIV-1 5′-UTR as a model, we could show that DDX3 is not required to assist the unwinding of secondary structures during ribosomal scanning as it could have been anticipated. In fact, DDX3 is associated within the eIF4F complex by an eIF4G–PABP (Poly A-binding protein cytoplasmic 1) double interaction but it is also able to directly bind to RNA. As such, DDX3 could be anchored to the 5′ terminus of the mRNA where it allows the entry of the eIF4F complex by performing local destabilization of RNA structures located close to the $m^7$GTP cap moiety. With the assistance of eIF4A, this complex unwinds 5′ terminal RNA structures to allow the entry of the 43S ribosomal subunit. Our results provide a rationale explanation on how some viral and cellular mRNAs that contain very stable RNA structures immediately at their 5′ extremity can still be efficiently translated by a cap-dependent ribosomal scanning mechanism.

## Results

### *DDX3 is required for translation of the HIV-1 gRNA*

Our initial goal was to analyse the role of DDX3 on HIV-1 gRNA translation. For this, we depleted DDX3 from HeLa cells by siRNA (Figure 1A) that we further transfected with a complete molecular clone HIV-1 NL4-3-Renilla (NL4-3R) developed in our laboratory. This encodes the entire HIV-1 genome modified in the Gag coding region to accommodate the *Renilla* luciferase reporter gene in order to quantify viral protein synthesis during the replication cycle (Soto-Rifo *et al*, 2012). Interestingly, accumulation of the gRNA in the cytoplasm was not affected after DDX3 knockdown indicating that the latter is not limiting for gRNA nuclear export under the knockdown conditions used in this manuscript (Supplementary Figure 1A, see left graph); this is in agreement with recent data showing that the concentration of DDX3 remaining after siRNA knockdown was sufficient to ensure HIV-1 gRNA export (Naji *et al*, 2012). However, we observed that HIV-1 translation was strongly repressed in DDX3-depleted cells indicating a critical role for the RNA helicase in this process (Figure 1B, compare siCtrl and siDDX3; Supplementary Figure 1A, right graph). It is noteworthy that the knockdown of DDX3 did not have any significant impact on global translation as evidenced by incorporation of $^{35}$S-methione on *de novo* synthesized proteins nor on the translational efficiency of a Renilla luciferase reporter gene (Supplementary Figures 1B and C), suggesting that DDX3 is not an essential factor for translation as previously proposed (Fukumura *et al*, 2003; Lai *et al*, 2008, 2010; Abaeva *et al*, 2011).

Ectopic expression of an siRNA resistant version of DDX3 (DDX3R in Figure 1B) fully restored HIV-1 translation ruling out the possibility of an off-target effect of the anti-DDX3 siRNA. Interestingly, a DDX3R mutant in the putative eIF4E-binding motif (Y38A/L43A in Figure 1B) as described (Shih *et al*, 2008) was as active as the wild-type protein indicating that DDX3 did not promote HIV-1 translation through the binding of the cap-binding protein.

DDX3 was proposed either to promote translation of mRNAs carrying complex 5′-UTRs by an ATP-dependent mechanism or to promote ribosomal subunit joining in an ATP-independent manner (Lai *et al*, 2008, 2010; Geissler *et al*, 2012). To discriminate between these two possibilities, we performed rescue experiments using DDX3R point mutants in motif I (K230E), motif II (DQAD) or the Q-motif (Q207A) as they are all involved in ATP binding and/or hydrolysis (Cordin *et al*, 2006). As observed, none of these mutants could reverse the inhibition of HIV-1 translation upon knockdown indicating that DDX3 promotes HIV-1 translation in an ATP-dependent manner (Figure 1B). However, we were surprised to observe that a mutation in motif III (S382L) was able to restore HIV-1 translation to the level of the control. Although the SAT motif III was suggested to link ATP hydrolysis with the unwinding activity (Cordin *et al*, 2006), the S382L point mutant of DDX3 (and its equivalent in Ded1) can still bind ATP while presenting limited unwinding activity suggesting that it may exhibit local strand separation but it would be unable to unwind RNA duplexes in a more processive manner (Yedavalli *et al*, 2004; Liu *et al*, 2008; Banroques *et al*, 2010). This is rather unexpected as it implies that DDX3 would not be needed for the unwinding of secondary structures during ribosomal scanning as it could have been anticipated. Such an assumption was strengthened by the fact that HIV-1 translation was not fully restored upon expression of a plasmid encoding the yeast Ded1 or human eIF4A RNA helicases (Figure 1C), which are expected to be more processive during ribosomal scanning (Berthelot *et al*, 2004; Marsden *et al*, 2006).

To further address a putative role for DDX3 in RNA secondary structures unwinding, we have transfected control or DDX3-depleted cells with a reporter mRNA in which translation of the Renilla luciferase was driven by the highly structured HIV-1 5′-UTR. As a control, we included a reporter mRNA harbouring the short and simple 5′-UTR from the human β-globin transcript (Supplementary Figure 1D). Consistent with a role of DDX3 in assisting translation of complex mRNAs, we observed that only HIV-1-driven translation (but not β-globin) was inhibited by DDX3 knockdown (Supplementary Figure 1D). This result further confirms that under our experimental conditions, DDX3 is not involved in the general process of translation initiation but rather, it promotes translation of complex mRNAs. Interestingly, increasing the stability of the HIV-1 5′-UTR by the insertion of an SL with a thermal stability of $-22.4$ kcal/mol at position 263 that inhibited translation by two-fold did not further impact the requirement for DDX3 (Supplementary Figure 1D). These data are very intriguing as they suggest a specific role for DDX3 in HIV-1 translation that appears not to be mediated through the unwinding of RNA secondary structures during ribosomal scanning as was shown for eIF4A (Svitkin *et al*, 2001; Pestova and Kolupaeva, 2002).

Thus, if DDX3 is not involved in ribosomal scanning or ribosomal subunit joining it could be required for an earlier event occurring most probably during cap structure recognition. Therefore, we reasoned that facilitating cap structure recognition by the introduction of an unstructured RNA spacer between the $m^7$GTP cap and the HIV-1 5′-UTR would abolish the need for DDX3. To investigate this, we have engineered synthetic transcripts in which the distance between the $m^7$GTP cap and the HIV-1 5′-UTR was lengthened by introducing 5, 10 or 20 repeats of the CAA triplet (see cartoon in Figure 1D). These constructs still possess the

 

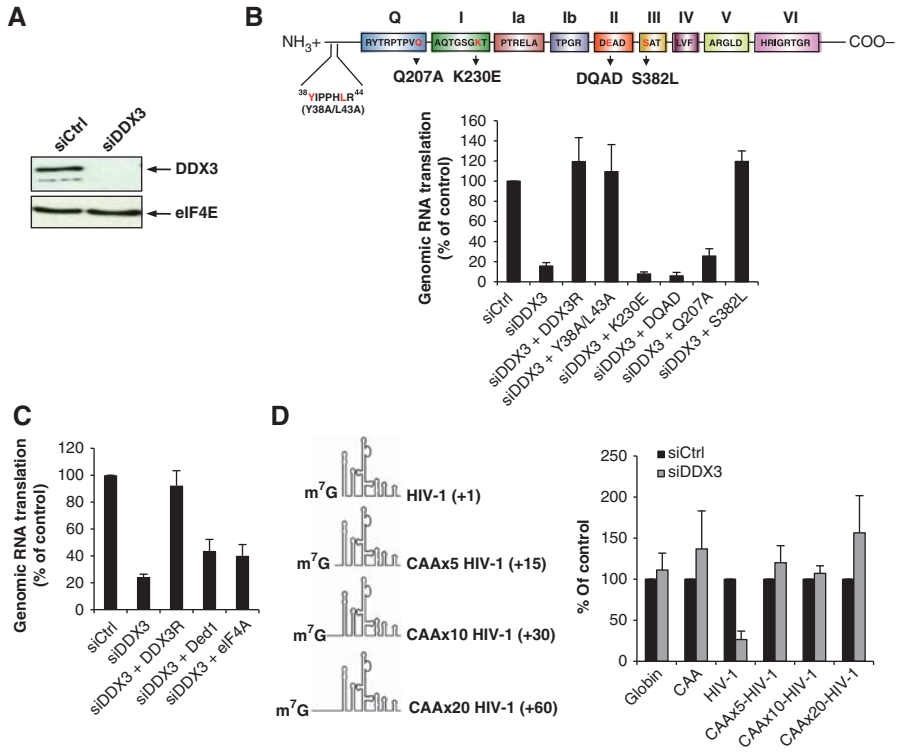


**Figure 1** DDX3 promotes translation of complex mRNAs. (**A**) Western blotting showing knockdown of DDX3 from HeLa cells transfected with a control siRNA (siCtrl) or an anti-DDX3 siRNA (siDDX3). eIF4E was used as a loading control. (**B**) Schematic representation of DDX3 helicase core indicating the sites that were mutated for functional analysis (upper cartoon). Control (siCtrl) and DDX3-depleted (siDDX3) HeLa cells were transfected with 0.3 μg of HIV-1-Renilla proviral DNA together 1 μg of a control vector coding for EGFP (in siCtrl and siDDX3). For rescue of siDDX3 cells, 1 μg of vectors encoding wild-type DDX3R or the indicated mutants were included. Translation of the HIV-1 genomic RNA (gRNA) was determined at 24 h.p.t. by reading the Renilla luciferase activity normalized to cytoplasmic gRNA levels. Results were normalized to the siCtrl/EGFP transfection (indicated as siCtrl in the figure, arbitrary set to 100%) and are presented as mean ± s.d. of three duplicated experiments. (**C**) Control (siCtrl) and DDX3-depleted (siDDX3) HeLa cells were transfected with 0.3 μg of HIV-1-Renilla proviral DNA together with 1 μg of vectors expressing EGFP (siCtrl and siDDX3) or DDX3R, yeast Ded1 or human eIF4A (in siDDX3). HIV-1 gRNA translation was determined at 24 h.p.t. by reading the Renilla luciferase activity normalized to cytoplasmic gRNA levels. Results were normalized to the siCtrl/EGFP DNA transfection (siCtrl in the figure, arbitrary set to 100%) and are presented as mean ± s.d. of three duplicated experiments. (**D**) Control (siCtrl) and DDX3-depleted (siDDX3) HeLa cells were transfected with 0.125 pmol of Renilla luciferase reporter mRNAs carrying the indicated 5′-UTR (see cartoon on the left). Renilla luciferase activity was analysed at 3 h.p.t. Results were normalized to siCtrl (arbitrary set to 100%) and are presented as mean ± s.d. of three duplicated experiments.

entire viral 5′-UTR, with the same free energy, GC content and RNA folding but they start with an unstructured spacer (Pestova and Kolupaeva, 2002). As controls Renilla luciferase reporter mRNAs carrying the β-globin 5′-UTR or 16 repeats of CAA were included. Remarkably, displacement of the HIV-1 5′-UTR by only 15 nucleotides (the length necessary to accommodate a 43S PIC) away from the cap completely abolished the need for DDX3 confirming that DDX3 is not involved in a mechanism requiring RNA unwinding as it is not needed once the 43S PIC has been engaged in ribosomal scanning.

### *DDX3 acts on a specific RNA motif that interferes with cap structure recognition*

In order to gain insights into the molecular mechanism by which DDX3 promotes translation, we continued to use translation driven by the HIV-1 5′-UTR as a model study case. This is justified by the fact that the structure of the 5′-UTR has been extensively characterized and modelled over the past years (Paillart *et al*, 2004; Wilkinson *et al*, 2008; Watts *et al*, 2009), which would facilitate the identification of specific RNA motifs involved in DDX3 activity.

The first question to answer was whether the need for DDX3 was a conserved feature among different members of the Retrovirus family. This is important since most Retroviruses contains an RHA-responsive PCE in their 5′-UTR (Bolinger and Boris-Lawrie, 2009). By using Renilla luciferase reporter mRNAs, we observed that translation of the Human immunodeficiency virus type-2 (HIV-2) and Simian immunodeficiency virus (SIV) was also sensitive to DDX3 knockdown (Figure 2A). This sharply contrasts with translation of the Feline immunodeficiency virus (FIV), Human T-cell lymphotropic virus (HTLV-I) and Murine Leukaemia virus (MLV), which were refractory to DDX3 depletion. Once again, it is noteworthy that absolutely all retroviral derived 5′-UTR are long, structured and GC rich (see Supplementary Figure 6A). This confirms that the presence of stable RNA secondary structures within the 5′-UTR did not determine the requirement for DDX3 and this must be due to the presence of a particular RNA feature that can be found and conserved among the primate lentiviruses HIV-1, HIV-2 and SIV. Consistent with this idea, the secondary structure of the 5′-UTR from the feline lentivirus FIV differs from that of primate lentiviruses (Kenyon *et al*, 2011). This

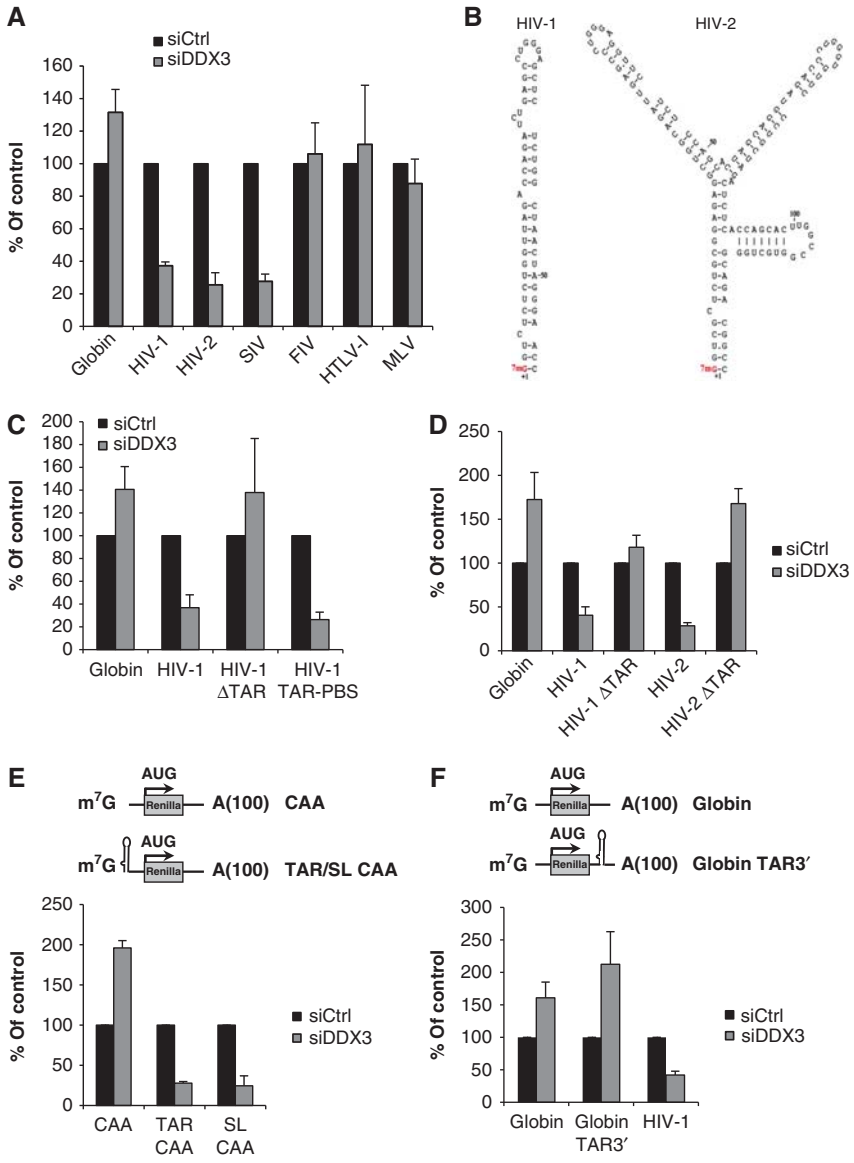


**Figure 2** DDX3 acts on structures located close to the $m^7$GTP cap. (**A**) Control (siCtrl) and DDX3-depleted (siDDX3) HeLa cells were transfected with 0.125 pmol of Renilla luciferase reporter mRNAs carrying the indicated 5′-UTR. Renilla luciferase activity was analysed at 3 h.p.t. Results were normalized to siCtrl (arbitrary set to 100%) and are presented as mean ± s.d. of three duplicated experiments. (**B**) Schematic representation of the HIV-1 and HIV-2 TAR structures. In HIV-1, the $m^7$GTP cap is base paired with the C residue at position 57 while in HIV-2 it is base paired with the C residue at position 123. (**C–E**) Control (siCtrl) and DDX3-depleted (siDDX3) HeLa cells were transfected with 0.125 pmol of Renilla luciferase reporter mRNAs carrying the indicated 5′-UTR. Renilla luciferase activity was analysed at 3 h.p.t. Results were normalized to siCtrl (arbitrary set to 100%) and are presented as mean ± s.d. of three duplicated experiments. (**F**) Control (siCtrl) and DDX3-depleted (siDDX3) HeLa cells were transfected with 0.125 pmol of the indicated Renilla luciferase reporter mRNA. Renilla luciferase activity was analysed at 3 h.p.t. Results were normalized to siCtrl (arbitrary set to 100%) and are presented as mean ± s.d. of three duplicated experiments.

result also confirms that DDX3 function could not be related to the activity of RHA on PCEs during ribosomal scanning (Hartman *et al*, 2006).

A hallmark of the 5′-UTR of primate lentiviruses is the presence of the TAR RNA motif, which is located immediately at position +1 of the mRNA (Berkhout, 2000). While this motif corresponds to a single SL in HIV-1, it forms a forked structure composed of three SLs in HIV-2 and SIV. As a consequence of TAR folding, the $m^7$GTP cap moiety is embedded within the structure through base pairing with a C residue located several dozens of nucleotides downstream (Figure 2B). As structures located close to the cap were shown to represent a strong barrier for attachment of eIF4F and the subsequent recruitment of the 43S PIC (Parkin *et al*, 1988; Kozak, 1989; Sagliocco *et al*, 1993; Pestova and Kolupaeva, 2002; Babendure *et al*, 2006), the TAR motif appears to be a likely candidate to justify the need for DDX3 activity. To investigate this, we have deleted TAR from the 5′ end of the HIV-1 5′-UTR (ΔTAR mRNA) together with a control deletion at the 3′ end part of the HIV-1 5′-UTR, as several SL structures are also present in this region (Supplementary Figure 2A). Transfection of the resulting reporter Renilla mRNAs in control and DDX3-depleted cells revealed that deletion of TAR completely abolished the requirement for DDX3 (Figure 2C, see ΔTAR) whereas deletion of other structured regions of the HIV-1 5′-UTR had no

 

impact (see TAR-PBS mRNA). Such data were confirmed by deletion of TAR from the HIV-2 5′-UTR, suggesting that the presence of this RNA structure at the 5′ end determines the requirement for DDX3 (Figure 2D).

To confirm this, we have inserted the HIV-1 TAR structure (nts 1–57 of the HIV-1 5′-UTR) at the 5′ terminal extremity of a synthetic reporter mRNA. In order to avoid any possible interaction between TAR and non-specific sequences in the 5′-UTR of the reporter gene, we have chosen to use CAA repeats for the remainder of the 5′-UTR. Interestingly, while translation of the CAA mRNA was not inhibited and rather stimulated by DDX3 knockdown, the addition of TAR switched towards a DDX3-dependent mechanism (Figure 2E). Because TAR is known to bind many cellular proteins (Bannwarth and Gatignol, 2005), we wanted to check whether dependence on DDX3 was due to some specific feature of TAR or if it could be triggered by any RNA structure placed at the 5′ end. This is why we have engineered an SL structure of random sequence that is not related to any viral TAR and whose predicted stability is even lower than that of HIV-1 TAR (Supplementary Figure 2B).

Interestingly, the insertion of this SL at the 5′ end of the CAA mRNA was sufficient to render it dependent on the presence of DDX3 (Figure 2E). This indicates that the requirement for DDX3 is not given by specific RNA sequences of viral origin nor to the binding of specific cellular proteins but is due to the presence of a stable hairpin loop at the 5′ end of the mRNA. It is noteworthy that some other helicases may also be recruited for the unwinding of the SL.

Another possibility that could explain the need for DDX3 would be an indirect effect by activation of the PKR pathway (Edery *et al*, 1989) or the generation of miRNAs due to processing of TAR by the RISC machinery (Ouellet *et al*, 2008). To check these hypotheses, we have inserted the TAR structure at the 3′ end of the globin-Renilla luciferase reporter mRNA that was transfected in control and DDX3-depleted cells (Figure 2F). However, the presence of TAR at this position had no effect whatsoever in the requirement for DDX3 indicating that its requirement is determined by the presence of the structure at the 5′ end of its target mRNAs. Thus, these results suggest that the presence of an RNA structure immediately at the 5′ end of a given mRNA is sufficient to render translation dependent on DDX3.

### *DDX3 binds to RNA in a non-specific manner*

Given its low affinity for RNA (Lorsch and Herschlag, 1998a, b), the RNA helicase eIF4A could only be recruited to the mRNA as a component of eIF4F upon cap structure recognition (Parsyan *et al*, 2011). As data above suggest that DDX3 acts on RNA structures located at the 5′ end of the mRNA that interfere with cap structure recognition by eIF4F, we reasoned that unlike eIF4A, DDX3 must be able to bind directly its RNA targets. As we have identified the HIV-1 TAR RNA as a natural target for DDX3 activity during translation, we examined whether recombinant DDX3 (rDDX3) could interact with a [$^{32}$P]-TAR RNA *in vitro*. In fact, incubation of TAR with rDDX3 resulted in the formation of high molecular weight complexes (Figure 3A, lanes 4–6). Addition of ATP (lane 5) or AMP-PNP (lane 6) to the binding reactions did not change the ability of DDX3 to bind TAR indicating that DDX3 could bind its RNA targets in an ATP-independent manner. This was further confirmed by the ability of the K230E mutant to bind to the HIV-1 5′-UTR (data not shown). Nevertheless, we cannot rule out the possibility that small amounts of ATP coming from our protein or RNA preparations are sufficient to stimulate binding. Consistent with its low affinity for RNA (Lorsch and Herschlag, 1998a, b), recombinant eIF4A was not able to bind TAR under our experimental conditions (lanes 7–9).

DEAD-box helicases bind to RNA through the sugar backbone and thus, binding is non-specific at least *in vitro* (Bono *et al*, 2006; Sengoku *et al*, 2006). This prompted us to examine whether RNA binding by DDX3 was also non-specific. In fact, we observed that DDX3 could bind the HIV-1 5′-UTR regardless of the presence of TAR (Figure 3B). As the HIV-1 5′-UTR is composed of several biologically functional SL RNA motifs (Supplementary Figure 3A), we wanted to map putative additional binding sites at the nucleotide resolution by toeprinting. It should be mentioned that, under our experimental conditions, any toeprint corresponding to DDX3 bound to TAR would be masked by the full-length signal due to its position at the very 5′ end. However, we repeatedly detected two specific toeprints downstream to TAR (Figure 3C, see toeprint #1 and #2 and Supplementary Figure 3A). The presence of these additional binding sites could be in agreement with the local strand separation mechanism proposed for DEAD-box proteins in which the binding close to the target duplex RNA would be a way to increase the loading of the protein and to stimulate unwinding (Yang and Jankowsky, 2006; Yang *et al*, 2007). Due to the lack of eIF4G (de Breyne *et al*, 2009) and its inability to bind to the HIV-1 5′-UTR, no toeprints were observed with eIF4A (data not shown).

To our surprise, DDX3 was also able to bind different 5′-UTRs including globin and HTLV-I (Figure 3D) for which we clearly showed that translation does not rely on DDX3. As observed above, recombinant eIF4A was unable to bind any of the 5′-UTRs. In order to further investigate the specificity of DDX3 binding, we have competed out the DDX3-HIV-1 5′-UTR interaction with an excess of cold ssRNAs or dsRNAs and this showed that ssRNAs were better competitors than dsRNAs (Supplementary Figure 3B and C).

Taken together, these *in-vitro* biochemical assays reveal that DDX3 has the ability to bind to the 5′-UTR irrespectively to its role in promoting, or not, translation of these given transcripts. However, it is also noteworthy that toeprinting reveals the presence of, at least, two specific motifs in the HIV-1 5′-UTR that are bound by DDX3.

### *DDX3 cooperates with eIF4A during TAR unwinding*

Given the ability of DDX3 to bind and act on TAR (Figures 2C and 3A), its most likely function during translation would be to catalyse the ATP-dependent remodelling of this RNA motif. Although it is well known from previous work that DDX3 is able to unwind short RNA duplexes *in vitro* (Yedavalli *et al*, 2004; Garbelli *et al*, 2011), we reasoned that DDX3 would only be able to locally destabilize TAR as the latter has more than two helical turns. Therefore, we have developed a system to monitor TAR unwinding in a cellular context. For this, we have engineered a TAR-Renilla mRNA (named TAR wt, see Supplementary Figure 4), which does not contain an AUG initiation codon and thus, only produces background levels of protein product (Figure 4A). However, the introduction of a single nucleotide mutation (C29A) in the loop of TAR

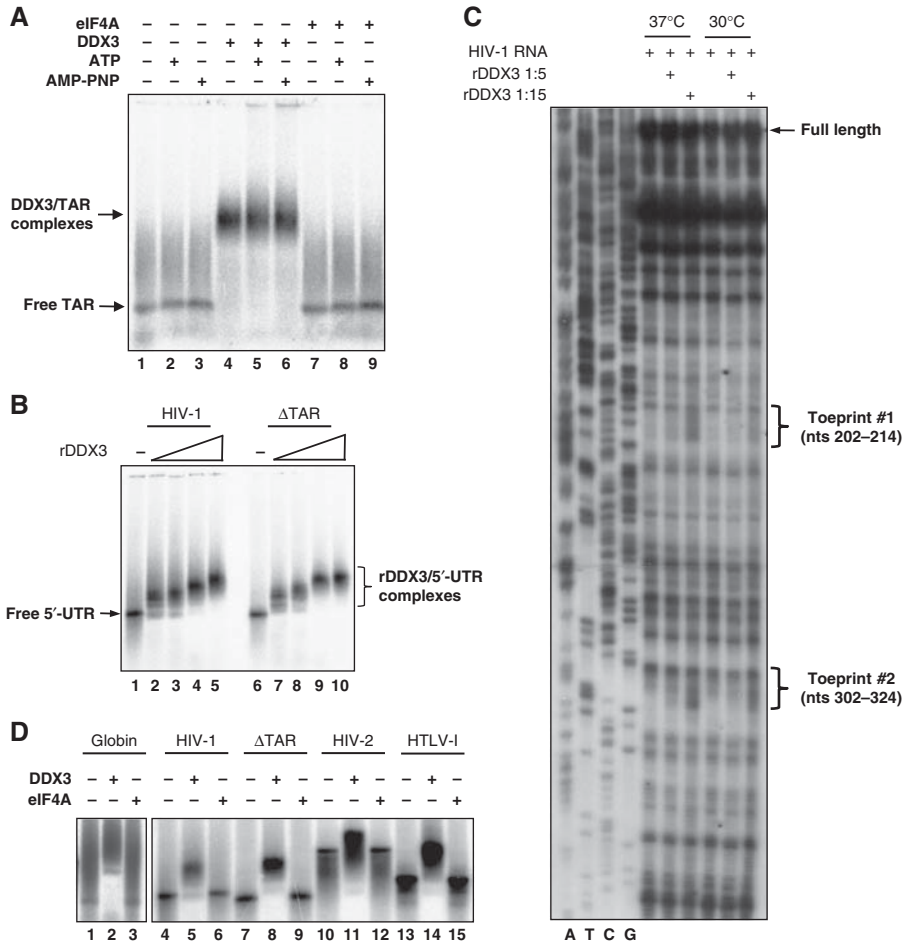


**Figure 3** DDX3 binds RNA in a non-specific manner. (**A**) 1.5% agarose gel showing results from an EMSA. *In vitro* transcribed, [$^{32}$P]-labelled TAR RNA was incubated in buffer (lanes 1–3), recombinant DDX3 (lanes 4–6) or eIF4A (lanes 7–9) in the absence (lanes 1, 4 and 7) or presence of ATP (lanes 2, 5 and 8) or AMP-PNP (lanes 3, 6 and 9). TAR and TAR/DDX3 complexes are indicated at the left of the image. Binding reactions were carried out at a 1:12 RNA:protein ratio. Result shown is representative of at least three independent experiments. (**B**) 1.5% agarose gel showing results from an EMSA. *In vitro* transcribed, [$^{32}$P]-labelled HIV-1 5′-UTR or ΔTAR 5′-UTR was incubated in buffer (lanes 1 and 6) or with increasing amounts of rDDX3 (lanes 2–5 and 7–10). The free RNA is indicated on the left and the RNA/DDX3 complexes are indicated at the right. Binding reactions were carried out at 1:0.2 (lanes 2 and 7); 1:0.6 (lanes 2 and 8); 1:3 (lanes 4 and 9) and 1:6 (lanes 5 and 10) RNA:protein ratio. Results shown are representative of at least three independent experiments. (**C**) Toeprints reactions preformed at 30 or 37°C were resolved as indicated in Materials and methods. Positions of two binding sites are indicated at the right. Their positions within the overall 5′-UTR structure are shown in Supplementary Figure 3. The image shown is representative of results obtained in three independent experiments. (**D**) 1.5% agarose gel showing results from an EMSA. *In vitro* transcribed, [$^{32}$P]-labelled 5′-UTR was incubated in buffer (lanes 1, 4, 7, 10 and 13), with recombinant DDX3 (lanes 2, 5, 8, 11 and 14) or with recombinant eIF4A (lanes 3, 6, 9, 12 and 15). Only DDX3 is able to form complexes with RNA. Binding reactions were carried at a 1:1.5 RNA:protein ratio. Results shown are representative of at least three independent experiments. Binding with the globin RNA was carried out in the same experiment but run in a different gel. Figure source data can be found with the Supplementary data.

that should not influence its structure, as it is not in a nucleotide paired region, creates an in-frame AUG codon (TAR-AUG) that can be used to synthesize the downstream luciferase reporter gene. Therefore, the reading of luciferase activity indicates that TAR unwinding has occurred in the system. From a functional point of view, insertion of this AUG results in a 20-fold increase in Renilla luciferase synthesis to a level comparable to the positive control which consists of the same reporter gene in which the TAR stem was destabilized by replacement of the 5′ branch with CAA repeats (see CAA-AUG-TAR in Supplementary Figure 4). Such an increase is due to initiation at the AUG codon embedded within the SL and that can only be reached by the 43S PIC if TAR gets unwound (Figure 4A, left graph). Thus, to assess the role of DDX3 in this process, we have performed these experiments in control or siDDX3-treated cells in the presence of the HIV-1 and globin controls. Interestingly, translation of the TAR-AUG mRNA was compromised by DDX3 knockdown indicating that the RNA helicase is required for TAR unwinding in cells (Figure 4A, right graph). As was expected, translation of the destabilized CAA-AUG-TAR mRNA did not show any level of dependence towards DDX3.

From results presented above, it could be speculated that DDX3 could either substitute or synergize with eIF4A during HIV-1 translation by destabilizing TAR. Indeed, eIF4A is the prototype for DEAD-box RNA helicases whose function in translation is thought to both participate in ribosome binding and scanning (Parsyan *et al*, 2011). Thus, we blocked eIF4A activity by treating HeLa cells with the highly specific eIF4A inhibitor hippuristanol (Bordeleau *et al*, 2006) and we looked at translation driven by a spectrum of 5′-UTRs including globin, HCV, HIV-1, TAR-AUG and CAA-TAR-AUG in these

 

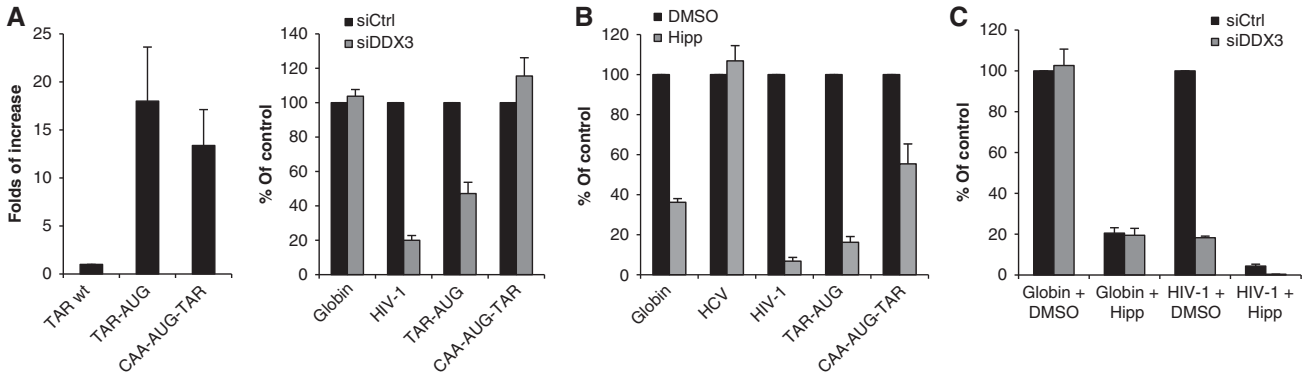


**Figure 4** DDX3 cooperates with eIF4A during TAR unwinding. (**A**) Indirect TAR unwinding assay *ex vivo*. Control (siCtrl) or DDX3-depleted (siDDX3) HeLa cells were transfected with 0.125 pmol of the indicated Renilla luciferase reporter mRNA and Renilla luciferase activity was analysed at 3 h.p.t. Efficiency of TAR unwinding (as determined by the Renilla luciferase activity) in siCtrl cells is showed on the left graph. The effect of DDX3 knockdown in TAR unwinding is showed on the right graph. Results were normalized to TAR wt (left, arbitrary set to 1; where average RLU for TAR wt, TAR-AUG and CAA-TAR-AUG are 7098, 126 461 and 111 792, respectively) or the siCtrl transfection (right, arbitrary set to 100%) and are presented as mean ± s.d. of three duplicated experiments. (**B**) HeLa cells previously treated with DMSO or 200 nM hippuristanol for 2 h were transfected with 0.125 pmol of the indicated Renilla luciferase reporter mRNA and Renilla luciferase activity was analysed at 3 h.p.t. Results were normalized to DMSO (arbitrary set to 100%) and are presented as mean ± s.d. of three duplicated experiments. (**C**) Control (siCtrl) or DDX3-depleted (siDDX3) HeLa cells were treated with DMSO or hippuristanol as described above and then transfected with 0.125 pmol of the indicated Renilla luciferase reporter mRNA and Renilla luciferase activity was analysed at 3 h.p.t. Results were normalized to siCtrl/DMSO condition (arbitrary set to 100%) and are presented as mean ± s.d. of three duplicated experiments. Normalized values obtained for HIV-1 under siCtrl/DMSO, siCtrl/Hipp, siDDX3/DMSO and siDDX3/Hipp are 100, 4, 18 and 0.4%, respectively.

cells (Figure 4B). Translation of all these constructs, with the exception of HCV (which does not require eIF4A for translation; Pestova *et al*, 1998) was severely impaired by the addition of hippuristanol. This implies that eIF4A is an essential factor for HIV-1 translation and suggests that DDX3 and eIF4A play distinct roles in translation initiation. This is particularly evidenced with translation of globin and CAA-AUG-TAR mRNAs, which are DDX3 independent but eIF4A dependent whereas HIV-1 and TAR-AUG constructs are dependent on both RNA helicases (Figures 4A and B). This double dependence suggests that the DDX3 and eIF4A may have additive effects on translation initiation. To verify this, we have added hippuristanol to DDX3-depleted cells and looked at translation driven by the globin or the HIV-1 5′-UTR. Remarkably, whereas addition of hippuristanol was drastically inhibitory to protein synthesis from both mRNAs, the additional knockdown of DDX3 only further affected HIV-1 translation with an additive effect to hippuristanol (Figure 4C). Such a result confirms that eIF4A and DDX3 exert different roles in translation with the latter being only needed for selected transcripts whereas eIF4A fulfills the role of an essential initiation factor.

### *DDX3 is associated with eIF4F for translation of complex mRNAs*

As DDX3 appears to be needed to promote the initial steps of ribosome binding on mRNAs harbouring secondary structures at their 5′ termini, we reasoned that it could be involved in the process of cap recognition and initial 43S PIC binding. Interestingly, while this work was in progress Lorsch and colleagues have shown that the binding of eIF4F to mRNAs is greatly facilitated by the presence of a free 5′ end (Rajagopal *et al*, 2012). Along this line, DDX3 has been shown to interact with several translation initiation factors (Lai *et al*, 2008; Lee *et al*, 2008; Shih *et al*, 2008, 2011), suggesting that DDX3 could be an active component of the translation initiation machinery.

Thus, we first looked at a possible colocalization of DDX3 with components of the translation initiation machinery. For this, we induced an oxidative stress in HeLa cells expressing a GFP–DDX3 fusion protein together with different HA-tagged members of the eIF4 group. Confocal microscopy analyses revealed that DDX3 was found together with eIF4F components eIF4E, eIF4G, eIF4A but also eIF4B and PABP in cytoplasmic stress granules, confirming its ability to be associated with the translation initiation machinery under these conditions (Figure 5A). However, we wanted to go further and search for any physical interaction between DDX3 and some of the eIF4F components in non-stressed cells. By performing immunoprecipitation from HeLa cells expressing HA–DDX3, we observed that eIF4G and PABP but not other members of eIF4F were associated with DDX3 (Figure 5B). This suggests that DDX3 has the ability to associate with PABP and eIF4G. To validate such a hypothesis, S7 nuclease-treated HeLa cells extracts were passed through an $m^7$GTP Sepharose affinity matrix and, after extensive washes, the resin was eluted and the bound material was revealed by western blotting. Interestingly, DDX3 was retained together with eIF4E, eIF4G and PABP on the $m^7$GTP affinity matrix further confirming the presence of DDX3 together with eIF4F components in an RNA-independent manner (Figure 5C, left panels). Retention was specific for eIF4F components as pre-incubation of cell extracts with $m^7$GpppG cap analogue completely abolished eIF4E and DDX3 retention (Figure 5C, right panel). Then, we wanted to determine whether interaction between DDX3 and eIF4G was direct or mediated by PABP. For this, we have carried out a GST-pull down assay in the rabbit reticulocyte lysate using *in-vitro* translated fragments of eIF4G and recombinant GST-DDX3 (Supplementary Figure 5). These data reveal that DDX3 interacts both with PABP and with the middle domain of eIF4G (682–1086) but not with the amino-terminus of eIF4G (1–681). This is particularly interesting as it suggests that the DDX3–eIF4G interaction is direct and not mediated

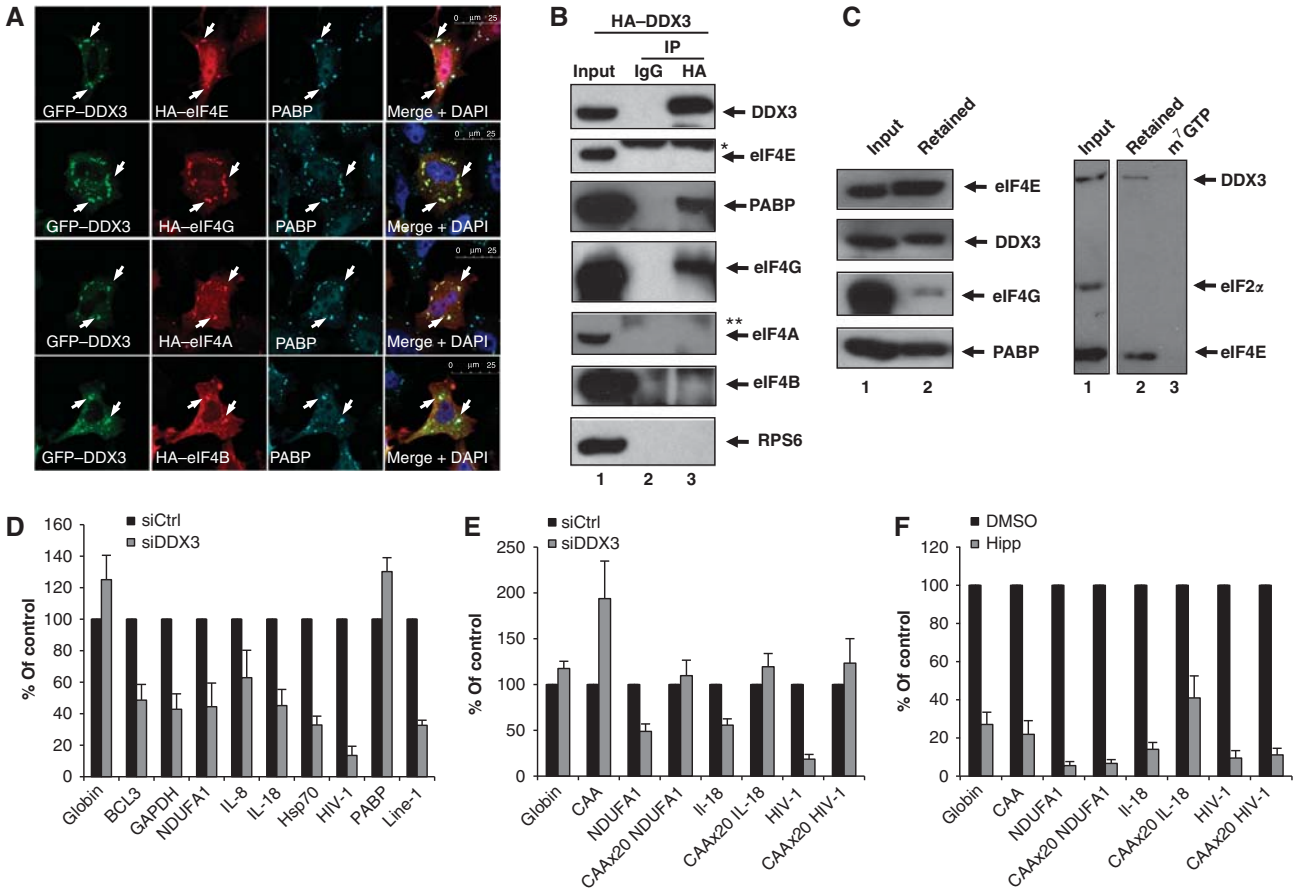


**Figure 5** DDX3 is associated with eIF4F and plays a role before ribosomal scanning. (**A**) HeLa cells transfected with vectors coding for GFP-DDX3 and the indicated eIF4F member were treated with 0.5 mM sodium arsenite for 45 min and then fixed and subjected to indirect immunofluorescence and confocal microscopy analyses. White arrows indicate colocalization between GFP-DDX3, HA-tagged eIF4F components and endogenous PABP in cytoplasmic stress granules. Scale bars 25 μm. (**B**) HeLa cells expressing HA-tagged DDX3 were subjected to IP using mouse IgG (lane 2) or a mouse anti-HA antibody (lane 3) and associated proteins were analysed by western blotting. Input (lane 1) corresponds to a 1/10 of the total cell extract. The asterisk (*) and the double asterisk (**) in the eIF4E and eIF4A panels show cross-reactivity of the anti-rabbit secondary antibody with the mouse IgG light chain and heavy chain, respectively. Bands observed upper and lower eIF4B in lanes 2 and 3 most probably correspond to unspecific recognition of our anti-goat secondary antibody. (**C**) S7 nuclease-treated HeLa cell extracts (100 μg) were incubated with an $m^7$GTP cap affinity matrix. Proteins retained after washing were analysed by western blotting (lane 2 in left panels). In the right panel, cell extracts were incubated in the absence or presence of $m^7$GpppG cap analogue (lanes 2 and 3, respectively) and proteins retained after washing were analysed by western blotting. Input (lane 1 in each panel) corresponds to 100 μg of cell extract. Bands shown in each panel correspond to the same western blot and were cropped for simplicity. (**D**, **E**) Control (siCtrl) and DDX3-depleted (siDDX3) or DMSO and Hippuristanol-treated HeLa cells were transfected with 0.125 pmol of the indicated Renilla luciferase reporter mRNA. Renilla luciferase activity was analysed at 3 h.p.t. Results were normalized to siCtrl (set to 100%) and are presented as mean ± s.d. of three independent experiments. (**F**) HeLa cells previously treated with DMSO or 200 nM hippuristanol for 2 h were transfected with 0.125 pmol of the indicated Renilla luciferase reporter mRNA and Renilla luciferase activity was analysed at 3 h.p.t. Results were normalized to DMSO (arbitrary set to 100%) and are presented as mean ± s.d. of three duplicated experiments. Figure source data can be found with the Supplementary data.

by PABP as the middle fragment of eIF4G does not contain the PABP binding site. Although the interaction between DDX3 and PABP has already been described (Shih *et al*, 2011), the binding of DDX3 to eIF4GI was not. However, Ded1 was recently shown to interact with the C-terminal RNA3 region of eIF4GI in yeast (Hilliker *et al*, 2011), suggesting an evolutionary conserved interaction.

The association of DDX3 with eIF4F together with its ability to bind RNA in a non-specific manner suggests that a likely function for DDX3 could be to promote the entry of eIF4F to the 5′ end of mRNAs, which would be accompanied by the local remodelling of the 5′ end of the transcript to promote 43S PIC entry. This is supported by the fact that DDX3 is at least required for translation of the HIV-1 gRNA (Figure 1) and the cyclin E1 transcript (Lai *et al*, 2010). This prompted us to look whether DDX3 was a specific factor for HIV-1 translation or if it could be needed for other cellular mRNAs. For this, we have created a set of Renilla luciferase reporter mRNAs in which translation was driven by the 5′-UTR of several cellular transcripts that are expected to be complex due to their length, GC content or both (Supplementary Figure 6A). As such, all transcripts used in this study were translated side by side in HeLa cells in order to compare their relative efficiency (Supplementary Figure 6B).

Transfection of control and DDX3-depleted cells revealed that siDDX3 impacted most of the selected complex 5′-UTRs tested with the exception of β-globin and PABP (Figure 5D). Given the fact that the PABP 5′-UTR is long and GC-rich (as that of FIV, HTLV-I and MLV), this result further confirms that specific RNA motifs, most probably located close to the cap moiety, rather than the complexity of the 5′-UTR *per se*

 

determine the involvement of DDX3 in translation initiation. To finally validate that RNA motifs located close to the cap structure determine the requirement for DDX3, we used some of the DDX3-sensitive 5′-UTRs derived from cellular transcripts that we characterized above and we inserted the 20 CAA repeats between the cap structure and the beginning of their 5′-UTR. As evidenced for HIV-1, insertion of CAA triplets between the $m^7$GTP cap and the NDUFA1 and IL-18 5′-UTRs also abolished the requirement for DDX3 indicating the conservation of the mechanism in DDX3-dependent cellular transcripts (Figure 5E). Once again, inactivation of eIF4A activity by hippuristanol inhibited translation of all mRNAs tested further confirming its general function in translation initiation (Figure 5F). Taken together, these results show that DDX3 is needed for translation of selected transcripts by acting prior to 43S ribosomal scanning.

## Discussion

Almost all aspects of RNA metabolism from transcription to decay involve the activity of DEAD-box proteins, a large family of RNA helicases that use ATP to destabilize RNA duplexes and remodel RNP complexes or to act as immobile RNA clamps to nucleate the assembly of large macromolecular complexes (Linder and Jankowsky, 2011). Despite the high structural conservation of the catalytic core, DEAD-box proteins play non-redundant functions within the cell and thus, macromolecular assemblies such as the spliceosome or the nuclear export and translation initiation machineries hold more than one RNA helicase to accomplish their activities. For instance, the eukaryotic translation initiation apparatus uses the DEAD-box proteins eIF4A, Ded1 (in yeast) and DHX29 in mammals in order to resolve the structural constraints encountered during 43S ribosomal scanning (Parsyan *et al*, 2011). Recently, Parker and colleagues have shown that the yeast homologue of DDX3, Ded1, was involved in general translation by promoting the formation and resolution of a complex between eIF4F and the mRNA (Hilliker *et al*, 2011).

Several cellular and viral transcripts possess structures located at the very 5′ end that strongly reduce the accessibility of the $m^7$GTP cap structure and, as a consequence, reduce 43S PIC binding. The best-characterized example is the HIV-1 gRNA, which commences with a highly stable 57 nucleotides SL motif that acts as a transcriptional enhancer (Berkhout, 2000). Despite this structural constraint, we, and others, have recently shown that the HIV-1 gRNA was efficiently translated in cells by a 5′ end cap-dependent mechanism (Berkhout *et al*, 2011; Soto-Rifo *et al*, 2012).

By using the HIV-1 5′-UTR as a model, we have fully investigated the molecular mechanism by which the cellular translational apparatus can deal with an SL structure at the vicinity of the $m^7$GTP cap and we found that this involves the intervention of the DEAD-box RNA helicase DDX3 that is used in a specific and time-dependent manner. Data presented here are in agreement with results published by the Tarn and Pestova groups proposing that DDX3 is not involved in general translation (Lai *et al*, 2008, 2010; Abaeva *et al*, 2011). Rather, we found that DDX3 promotes translation driven by complex 5′-UTRs derived from a subset of viral and cellular mRNAs carrying a 5′ proximal SL structures. By performing *in-vitro* biochemical assays, we gained evidence that DDX3 can directly bind its target RNA duplex (Figure 3). Interestingly, we could also characterize two DDX3 binding sites on the HIV-1 5′-UTR that correspond to single-stranded regions (Figure 3). This confirms the ability of DEAD-box RNA helicases to bind RNA non-specifically through the sugar phosphates (Bono *et al*, 2006; Sengoku *et al*, 2006) but it could also give biological significance to the proposed mechanism of local strand separation in which binding close to the target RNA duplex would be used as loading platforms (Yang and Jankowsky, 2006; Yang *et al*, 2007).

In cells, we have obtained evidence suggesting that DDX3 could be preferentially used to locally unwind the base of the TAR motif in a function that cannot be fulfilled by other related RNA helicases such as eIF4A (Figures 1 and 4). Local destabilization rather than complete unwinding mediated by DDX3 is favoured by the fact that translation of HIV-1 and HIV-2, which possess TAR structures with high differences in length, stability and effects on translation (Soto-Rifo *et al*, 2012), were similarly dependent on DDX3 (Figure 2).

Besides its RNA binding properties, we also show that DDX3 is associated with the eIF4F complex through an eIF4G and PABP double interaction in an RNA-independent manner (Figure 5). Therefore, it suggests that DDX3 can be delivered to the target mRNA either by direct binding (Figure 3) or associated with components of eIF4F (Figure 5) or both. Given these data, it is tempting to speculate that DDX3 is a core constituent of eIF4F and becomes only required if it 'meets' an SL at the 5′ end of the mRNA. Such a hypothesis is in agreement with results presented in Figure 5 showing that introduction of an RNA spacer between the $m^7$GTP and the target RNA renders all tested transcripts resistant to DDX3 knockdown despite the fact that they remained highly sensitive to eIF4A inhibition by hippuristanol. Once again, this argues towards a specialized role for DDX3 in the translation of selected mRNAs whereas eIF4A is needed for all transcripts. Due to the inability of DEAD-box proteins to unwind RNA duplexes with more than two helical turns, it is more likely that DDX3 may only locally destabilize the RNA structure to generate a single-stranded region large enough to allow the recognition of the $m^7$GTP cap or loading onto the 40S subunit. As such, this fits well with recent data from the Lorsch group showing that entry of the eIF4F complex is greatly facilitated by the presence of a free 5′ end on the mRNA (Rajagopal *et al*, 2012). Alternatively, it may be possible that DDX3 reduces the 5′ RNA secondary structures and removes the proteins bound to the 5′ extremity to facilitate 43S ribosome binding. Then, the helicase activity of eIF4A (together with its co-factors eIF4B/4H), and perhaps DHX29, would be strong enough to accomplish RNA unwinding during ribosomal scanning. The understanding of how all these helicases are kinetically recruited and utilized during the early steps of translation will be a very interesting challenge for future work.

## Materials and methods

### *DNA constructs*

The pNL4-3-Renilla (NL4-3R) vector was previously described (Soto-Rifo *et al*, 2012). All pRenilla-derived constructs were obtained by inserting the selected region between the *Pvu*II-*Bam*HI sites of the pRenilla vector as previously described (Soto Rifo *et al*, 2007). The 5′-UTRs inserted in the pRenilla construct correspond to human β-globin (globin), B-cell CLL/lymphoma 3

(BCL3), glyceraldehyde-3-phospahte dehydrogenase (GAPDH), NADH dehydrogenase (ubiquinone) alpha subcomplex 1 (NDUFA1), Interleukin 8 (IL-8), Interleukin 18 (IL-18), heat-shock protein of 70 kDa 1A (Hsp70), PABP, long interspread nuclear element 1 (Line-1), HIV-1 and HIV-2, SIV, FIV, HTLV-I and Friend MLV. cDNAs for DDX3, Ded1 and eIF4A were inserted into the *Eco*RI/*Not*I sites of the pCIneo-HA vector previously described (Pillai *et al*, 2004). Site-directed mutagenesis of pCIneo-HA-DDX3 was carried out with the Quick change mutagenesis kit (Agilent Technologies). pET21-DDX3 was obtained by inserting the DDX3 cDNA into *Xho*I-*Nde*I sites of the pET21 vector. pET21-eIF4A vector was previously described (Pestova *et al*, 1998). pGST-DDX3 was obtained by subcloning the *Eco*RI/*Not*I fragment from the pCIneo-HA-DDX3 vector into the pGEX-6p vector. All DNA constructs were verified by sequencing.

### *In-vitro transcription*

Prior to *in vitro* transcription the desired pRenilla-derived vectors were linearized by *Eco*RI digestion to obtain a 100 nt-long poly (A) tail or with *Bam*HI to obtain the desired 5′-UTR for radiolabelling. *In-vitro* transcription was carried as previously described (Soto Rifo *et al*, 2007).

### *Cell culture, DNA, mRNA and siRNA transfections*

HeLa cells were maintained as described (Soto-Rifo *et al*, 2012). DNA transfection was carried out using JetPEI (Polyplus Transfection) as previously described (Soto-Rifo *et al*, 2012). mRNA transfection was carried using the Trans IT mRNA transfection kit (Mirus) as previously described (Dieterich *et al*, 2007; Soto-Rifo *et al*, 2012).

Control or DDX3 siRNAs (5′-GCAGCACGACUUCUUCAAGdTdT-3′ and 5′-GAUGCUGGCUCGUGAUUUCUdTdT-3′, respectively) were purchased from Eurogenetec, Inc and transfected at a 10 nM final concentration using Intereferin (Polyplus Transfection) following supplier's indications. At 48 h.p.t., DNA or mRNA transfections were carried as indicated above.

When indicated, cells were treated with 200 nM hippuristanol (or the equivalent volume of DMSO) during 3 h prior mRNA transfection.

For metabolic labelling, growing HeLa cells previously transfected with siRNAs were incubated in methionine-free medium (Gibco, BRL) for 30 min and then labelled with $^{35}$S-methionine (Perkin-Elmer) which was added for an additional 30 min. Cell extracts were subjected to 10% SDS–PAGE and quantification was performed by using a Fuji Phosphoimager and the Fuji FLA 5000 software (Fuji).

### *Renilla luciferase activity*

Renilla luciferase activity was measured using the Renilla Luciferase Assay System (Promega Co, Madison, WI, USA) in a Veritas Luminometer (Turner Biosystems) as previously described (Dieterich *et al*, 2007; Soto-Rifo *et al*, 2012).

### *Immunofluorescence and confocal microscopy*

HeLa cells were cultured in Lab-Tek Chamber Slides (Nunc) and maintained and transfected with 0.2 μg of pEGFP-DDX3 together with the HA-tagged DNA constructs as described above. Cells were washed twice with 1 × PBS and fixed for 10–15 min at room temperature with 4% paraformaldehyde, quenched for 5 min at room temperature with 50 mM $NH_4Cl$ and then permeabilized for 5 min at RT with 0.2% Triton X-100. Cells were blocked at RT with 1% BSA for 2–3 h. Mouse anti-HA (Covance) and rabbit anti-PABP (a kind gift from Dr Simon Morley, University of Sussex, UK) primary antibodies (1/100) in 1% BSA were added for 1–2 h at RT. After two washes with 1% BSA (15 min each), cells were incubated for 1 h with anti-mouse Alexa 545 and anti-rabbit Alexa 633 antibodies (Molecular Probes) diluted at 1/1000 in 1% BSA. Cells were washed twice for 15 min with 1% BSA, twice with 1 × PBS, incubated with Hoescht (1/10 000; Invitrogen Life Technologies) for 5 min at RT, washed twice for 5 min with 1 × PBS, twice with water and mounted with Fluoromount (Invitrogen Life Technologies). Images representative from hundreds of cells were obtained with a TCS SP5 AOBS Spectral Confocal Microscope (Leica Microsystems) and recovered and merged using the LAS AF Lite software (Leica Microsystems).

### *Co-immunoprecipitation and western blotting*

HeLa cells were transfected with the pCIneo-HA-DDX3 vector as indicated above. Co-IP was carried out as described (Lykke-Andersen *et al*, 2001). Briefly, transfected cells were washed with PBS, recovered by centrifugation at 2500 r.p.m. for 10 min at 4°C and resuspended in 400 μl of hypotonic gentle lysis buffer (10 mM Tris–HCl pH 7.5; 10 mM NaCl, 10 mM EDTA; 0.5% Triton X-100 and protease inhibitors cocktail). Cells were incubated for 10 min on ice, NaCl was adjusted to 150 mM and the lysate was cleared by centrifugation at 10 000 r.p.m. for 10 min at 4°C. The supernatant was incubated with 10 μg of a mouse anti-HA antibody (Covance) or 10 μg of mouse IgG (Millipore) for 3–4 h at 4°C, 10 r.p.m. rotation. Protein–antibody complexes were recovered with 50 μl of Dynabeads Protein G (Invitrogen) during 1 h at 4°C, 10 r.p.m. rotation and recovered complexes were washed extensively with NET-2 buffer (50 mM Tris–HCl pH 7.5; 150 mM NaCl; 0.05% Nonidet P40) and resuspended in 60 μl of SDS-loading buffer. In all, 30 μl aliquots were subject to 7.5 or 10% SDS–PAGE, transferred onto PVDF membrane and blotted using anti-DDX3 (Abcam), eIF4GI, PABP, eIF4A, eIF4E, eIF4B (kindly provided by Dr Simon Morley, University of Sussex, UK) or RPS6 antibodies as previously described (Soto-Rifo *et al*, 2012).

### *$m^7$GTP cap affinity matrix*

Cytoplasmic extracts from HeLa cells (100 μg of total protein) previously treated with S7 nuclease (Roche) were incubated for 10 min at 37°C in cap binding buffer (50 mM Tris–HCl pH 7.5; 30 mM NaCl; 1 mM DTT; 2.5 mM $MgCl_2$; 0.5% Glycerol) in the absence or presence of 5 mM $m^7$GpppG cap analogue (New England Biolabs) as control. Extracts were incubated overnight at 4°C with 15–20 μl of $m^7$GTP-Sepharose 4B (GE Healthcare) under gentle shaking. Retained proteins were washed three times with cap washing buffer (50 mM Hepes pH 7.5; 40 mM NaCl; 2 mM EDTA; 0.1% Triton), eluted by boiling in SDS-loading buffer and analysed by western blot as indicated above.

### *Purification of recombinant proteins*

*E. coli* BL21 cells expressing the pET21-DDX3 vector were grown until $A_{600}$ reached 0.6–0.8 and then, induced with 0.5 mM IPTG for 5 h at 15°C. Pellets were resuspended in native lysis buffer (50 mM $NaH_2PO_4$ pH 8.0; 300 mM NaCl and 10 mM imidazole) supplemented with 1 mg/ml Lysozyme (Sigma), 30 U/ml Nuclease S7 (Roche), 1 mM $CaCl_2$, 1% Triton X-100 and protease inhibitor cocktail (Roche). Cells were lysed with a French press at 1100 p.s.i. and cleared at 5000 *g* for 15 min. The supernatant was recovered and incubated with Ni-NTA resin (Qiagen) (previously equilibrated in native lysis buffer) at 4°C for at least 3 h under gentle shaking. The mixture was applied into a 2-ml column (Bio-Rad) and flow-through was obtained by gravity. The resin was then washed four times with five volumes of native washing buffer (50 mM $NaH_2PO_4$ pH 8.0; 300 mM NaCl and 20 mM imidazole) and protein was eluted with native elution buffer (50 mM $NaH_2PO_4$ pH 8.0; 300 mM NaCl; 500 mM imidazole and protease inhibitor cocktail). The protein was salt washed with (25 mM Tris-Cl pH 7.5, 50 mM NaCl, 0.1 mM $MgCl_2$, 25% glycerol and protease inhibitor cocktail) and concentrated using Spin-X UF Concentrators (Corning). Samples obtained during every step were analysed by 10% SDS–PAGE and Coomasie blue staining.

*E. coli* BL21 Star (DE3) cells were transformed with the pET21-eIF4A vector (Pestova *et al*, 1998). Expression of the recombinant protein was induced for 4 h with 0.5 mM IPTG when culture reach $0.4 < OD_{600} < 0.6$. After centrifugation of bacterial cultures, pellets were resuspended in 20 mM Tris–HCl pH 7.5, 300 mM KCl and 10% glycerol and then sonicated on ice. Supernatants derived from the bacterial lysate by centrifugation were added to a Ni-NTA column that has been prepared by adding 800 μl of a 50% Ni-NTA suspension (Qiagen) to a Bio-Rad Polyprep chromatography column. Washes and imidazole elutions were done according to the manufacturer. The eIF4A elution was then dialyzed and applied to an FPLC Hi-TrapQ column (GE Healthcare). Samples obtained during every step were analysed by 10% SDS–PAGE and Coomasie blue staining.

### *GST pull down*

The rabbit reticulocyte lysate (Promega) was programmed with RNAs coding for eIF4G fragments (1–681 or 682–1086) or PABP in the presence of [$^{35}$S]-methionine as described (Soto Rifo *et al*, 2007).

Translation reactions were treated with RNAse A and then incubated with GST or GST-DDX3 bound to Glutathione Sepharose 4B (GE Healthcare) during 2 h at 4°C. Retained material was washed three times with PBS and resolved by SDS–PAGE. Gels were dried and images acquired in a PhosphorImager FLA 5100 (Fuji).

### *EMSA*

[$^{32}$P]-UTP radiolabelled RNAs were obtained by *in-vitro* transcription as above but using 0.5 mM rNTPs (without rUTP), 12.05 μM rUTP and [α-$^{32}$P]-rUTP (40 μCi/reaction). RNAs were treated with 2 U of RQ1 RNase-free DNase (Promega), precipitated with three volumes of 100% Ethanol and purified using Ilustra Microspin G25 column (GE Healthcare).

In all, 0.044 pmol (4.4 nM) of [$^{32}$P]-RNA was incubated for 15 min at 37°C with recombinant DDX3 or eIF4A (or dialysis buffer as control) in binding buffer (30 mM Tris–HCl pH 7.0; 0.5 mM $MgCl_2$; 0.1 mM $ZnCl_2$; 50 mM NaCl) in the presence of 40 U/reaction of RNAsin (Promega). After incubation, samples were analysed on 1.5% Agarose TBE gels. Gels were dried and images acquired in a PhosphorImager FLA 5100 (Fuji).

### *Toeprint assay*

In all, 0.5 pmol of HIV-1 RNA was incubated for 15 min at 37°C in a 40-μl reaction volume that contained 1 mM DTT; 100 mM KCl; 20 mM Tris pH 7.5; 2.5 mM MgOAc, 40 U RNasin (Promega), recombinant DDX3 or eIF4A (2.5 and 7 pmol). [$^{32}$P]-labelled primer (nucleotides 416–440, HIV-1 NL4-3 strain) was added to the mixture for 5 min and chilled on ice. Primer extension analysis was done by adding 1 μl of MgOAc (360 mM), 4 μl of dNTPs (10 mM) and 5 units AMV-RT to reaction mixtures, followed by incubation for 60 min at 37 or 30°C. cDNAs were analysed by electrophoresis through 6% polyacrylamide sequencing gels.

### *Supplementary data*

Supplementary data are available at *The EMBO Journal* Online (http://www.embojournal.org).

## Acknowledgements

We thank Dr Jerry Pelletier (McGill University, Canada), Dr Simon Morley (University of Sussex, UK), Dr Tatyana Pestova and Dr Christopher Hellen (SUNY Downstate Medical Center, USA), Dr Madeleine Duc Dudon (ENS-Lyon), Dr Ramesh Pillai (EMBL Grenoble, France) and Dr Gael Cristofari (Université de Nice, France) for reagents. Pr JL Darlix and Dr A Cimarelli (ENS-Lyon) are acknowledged for helpful comments. We also wish to thank the 'Plateau Technique Imagerie/Microscopie (PLATIM) UMS3444 BioSciences Gerland-Lyon Sud' for assistance with confocal microscopy. RSR holds a CONICYT-Chile/French Embassy doctoral fellowship and is further supported by an Agence Nationale des Recherches sur le SIDA et les Hépatites Virales (ANRS) post-doctoral fellowship. PSR holds a 'Becas Chile/CONICYT' doctoral fellow and TL holds a 'Region Rhône Alpes' doctoral fellow and is further supported by the Fondation pour la Recherche Medicale (FRM). Work in our laboratory is supported by ANRS and a 'Contrat d'Interface' with the Hospices Civils de Lyon.

*Author contributions*: RSR and TO designed research and wrote the paper. RSR performed the experiments. PSR, TL, SdB and DD contributed with experimental procedures.

## Conflict of interest

The authors declare that they have no conflict of interest.

## References

Abaeva IS, Marintchev A, Pisareva VP, Hellen CU, Pestova TV (2011) Bypassing of stems versus linear base-by-base inspection of mammalian mRNAs during ribosomal scanning. *EMBO J* **30:** 115–129

Babendure JR, Babendure JL, Ding JH, Tsien RY (2006) Control of mammalian translation by mRNA structure near caps. *RNA* **12:** 851–861

Bannwarth S, Gatignol A (2005) HIV-1 TAR RNA: the target of molecular interactions between the virus and its host. *Curr HIV Res* **3:** 61–71

Banroques J, Doere M, Dreyfus M, Linder P, Tanner NK (2010) Motif III in superfamily 2 'helicases' helps convert the binding energy of ATP into a high-affinity RNA binding site in the yeast DEAD-box protein Ded1. *J Mol Biol* **396:** 949–966

Berkhout B (2000) Multiple biological roles associated with the repeat (R) region of the HIV-1 RNA genome. *Adv Pharmacol* **48:** 29–73

Berkhout B, Arts K, Abbink TE (2011) Ribosomal scanning on the 5′-untranslated region of the human immunodeficiency virus RNA genome. *Nucleic Acids Res* **39:** 5232–5244

Berthelot K, Muldoon M, Rajkowitsch L, Hughes J, McCarthy JE (2004) Dynamics and processivity of 40S ribosome scanning on mRNA in yeast. *Mol Microbiol* **51:** 987–1001

Bolinger C, Boris-Lawrie K (2009) Mechanisms employed by retroviruses to exploit host factors for translational control of a complicated proteome. *Retrovirology* **6:** 8

Bono F, Ebert J, Lorentzen E, Conti E (2006) The crystal structure of the exon junction complex reveals how it maintains a stable grip on mRNA. *Cell* **126:** 713–725

Bordeleau ME, Mori A, Oberer M, Lindqvist L, Chard LS, Higa T, Belsham GJ, Wagner G, Tanaka J, Pelletier J (2006) Functional characterization of IRESes by an inhibitor of the RNA helicase eIF4A. *Nat Chem Biol* **2:** 213–220

Bushman FD, Malani N, Fernandes J, D'Orso I, Cagney G, Diamond TL, Zhou H, Hazuda DJ, Espeseth AS, Konig R, Bandyopadhyay S, Ideker T, Goff SP, Krogan NJ, Frankel AD, Young JA, Chanda SK (2009) Host cell factors in HIV replication: meta-analysis of genome-wide studies. *PLoS Pathog* **5:** e1000437

Cordin O, Banroques J, Tanner NK, Linder P (2006) The DEAD-box protein family of RNA helicases. *Gene* **367:** 17–37

de Breyne S, Yu Y, Unbehaun A, Pestova TV, Hellen CU (2009) Direct functional interaction of initiation factor eIF4G with type 1 internal ribosomal entry sites. *Proc Natl Acad Sci USA* **106:** 9197–9202

Dieterich K, Soto Rifo R, Faure AK, Hennebicq S, Ben Amar B, Zahi M, Perrin J, Martinez D, Sele B, Jouk PS, Ohlmann T, Rousseaux S, Lunardi J, Ray PF (2007) Homozygous mutation of AURKC yields large-headed polyploid spermatozoa and causes male infertility. *Nat Genet* **39:** 661–665

Edery I, Petryshyn R, Sonenberg N (1989) Activation of double-stranded RNA-dependent kinase (dsl) by the TAR region of HIV-1 mRNA: a novel translational control mechanism. *Cell* **56:** 303–312

Fukumura J, Noguchi E, Sekiguchi T, Nishimoto T (2003) A temperature-sensitive mutant of the mammalian RNA helicase, DEAD-BOX X isoform, DBX, defective in the transition from G1 to S phase. *J Biochem* **134:** 71–82

Garbelli A, Beermann S, Di Cicco G, Dietrich U, Maga G (2011) A motif unique to the human DEAD-box protein DDX3 is important for nucleic acid binding, ATP hydrolysis, RNA/DNA unwinding and HIV-1 replication. *PLoS One* **6:** e19810

Geissler R, Golbik RP, Behrens SE (2012) The DEAD-box helicase DDX3 supports the assembly of functional 80S ribosomes. *Nucleic Acids Res* **40:** 4998–5011

Hartman TR, Qian S, Bolinger C, Fernandez S, Schoenberg DR, Boris-Lawrie K (2006) RNA helicase A is necessary for translation of selected messenger RNAs. *Nat Struct Mol Biol* **13:** 509–516

Hilliker A, Gao Z, Jankowsky E, Parker R (2011) The DEAD-box protein Ded1 modulates translation by the formation and resolution of an eIF4F-mRNA complex. *Mol Cell* **43:** 962–972

Imataka H, Sonenberg N (1997) Human eukaryotic translation initiation factor 4G (eIF4G) possesses two separate and independent binding sites for eIF4A. *Mol Cell Biol* **17:** 6940–6947

Jackson RJ, Hellen CU, Pestova TV (2010) The mechanism of eukaryotic translation initiation and principles of its regulation. *Nat Rev Mol Cell Biol* **11:** 113–127

Kenyon JC, Tanner SJ, Legiewicz M, Phillip PS, Rizvi TA, Le Grice SF, Lever AM (2011) SHAPE analysis of the FIV Leader RNA reveals a structural switch potentially controlling viral packaging and genome dimerization. *Nucleic Acids Res* **39:** 6692–6704

Kozak M (1989) Circumstances and mechanisms of inhibition of translation by secondary structure in eucaryotic mRNAs. *Mol Cell Biol* **9:** 5134–5142

Kozak M (1991) Structural features in eukaryotic mRNAs that modulate the initiation of translation. *J Biol Chem* **266:** 19867–19870

Lai MC, Chang WC, Shieh SY, Tarn WY (2010) DDX3 regulates cell growth through translational control of cyclin E1. *Mol Cell Biol* **30:** 5444–5453

Lai MC, Lee YH, Tarn WY (2008) The DEAD-box RNA helicase DDX3 associates with export messenger ribonucleoproteins as well as tip-associated protein and participates in translational control. *Mol Biol Cell* **19:** 3847–3858

Lee CS, Dias AP, Jedrychowski M, Patel AH, Hsu JL, Reed R (2008) Human DDX3 functions in translation and interacts with the translation initiation factor eIF3. *Nucleic Acids Res* **36:** 4708–4718

Linder P, Jankowsky E (2011) From unwinding to clamping - the DEAD box RNA helicase family. *Nat Rev Mol Cell Biol* **12:** 505–516

Liu F, Putnam A, Jankowsky E (2008) ATP hydrolysis is required for DEAD-box protein recycling but not for duplex unwinding. *Proc Natl Acad Sci USA* **105:** 20209–20214

Lorsch JR, Herschlag D (1998a) The DEAD box protein eIF4A. 1. A minimal kinetic and thermodynamic framework reveals coupled binding of RNA and nucleotide. *Biochemistry* **37:** 2180–2193

Lorsch JR, Herschlag D (1998b) The DEAD box protein eIF4A. 2. A cycle of nucleotide and RNA-dependent conformational changes. *Biochemistry* **37:** 2194–2206

Lykke-Andersen J, Shu MD, Steitz JA (2001) Communication of the position of exon-exon junctions to the mRNA surveillance machinery by the protein RNPS1. *Science* **293:** 1836–1839

Marsden S, Nardelli M, Linder P, McCarthy JE (2006) Unwinding single RNA molecules using helicases involved in eukaryotic translation initiation. *J Mol Biol* **361:** 327–335

Naji S, Ambrus G, Cimermancic P, Reyes JR, Johnson JR, Filbrandt R, Huber MD, Vesely P, Krogan NJ, Yates 3rd JR, Saphire AC, Gerace L (2012) Host cell interactome of HIV-1 Rev includes RNA helicases involved in multiple facets of virus production. *Mol Cell Proteomics* **11:** M111.015313

Ouellet DL, Plante I, Landry P, Barat C, Janelle ME, Flamand L, Tremblay MJ, Provost P (2008) Identification of functional microRNAs released through asymmetrical processing of HIV-1 TAR element. *Nucleic Acids Res* **36:** 2353–2365

Paillart JC, Dettenhofer M, Yu XF, Ehresmann C, Ehresmann B, Marquet R (2004) First snapshots of the HIV-1 RNA structure in infected cells and in virions. *J Biol Chem* **279:** 48397–48403

Parkin NT, Cohen EA, Darveau A, Rosen C, Haseltine W, Sonenberg N (1988) Mutational analysis of the 5′ non-coding region of human immunodeficiency virus type 1: effects of secondary structure on translation. *EMBO J* **7:** 2831–2837

Parsyan A, Shahbazian D, Martineau Y, Petroulakis E, Alain T, Larsson O, Mathonnet G, Tettweiler G, Hellen CU, Pestova TV, Svitkin YV, Sonenberg N (2009) The helicase protein DHX29 promotes translation initiation, cell proliferation, and tumorigenesis. *Proc Natl Acad Sci USA* **106:** 22217–22222

Parsyan A, Svitkin Y, Shahbazian D, Gkogkas C, Lasko P, Merrick WC, Sonenberg N (2011) mRNA helicases: the tacticians of translational control. *Nat Rev Mol Cell Biol* **12:** 235–245

Pestova TV, Kolupaeva VG (2002) The roles of individual eukaryotic translation initiation factors in ribosomal scanning and initiation codon selection. *Genes Dev* **16:** 2906–2922

Pestova TV, Shatsky IN, Fletcher SP, Jackson RJ, Hellen CU (1998) A prokaryotic-like mode of cytoplasmic eukaryotic ribosome binding to the initiation codon during internal translation initiation of hepatitis C and classical swine fever virus RNAs. *Genes Dev* **12:** 67–83

Pickering BM, Willis AE (2005) The implications of structured 5′ untranslated regions on translation and disease. *Semin Cell Dev Biol* **16:** 39–47

Pillai RS, Artus CG, Filipowicz W (2004) Tethering of human Ago proteins to mRNA mimics the miRNA-mediated repression of protein synthesis. *RNA* **10:** 1518–1525

Pisareva VP, Pisarev AV, Komar AA, Hellen CU, Pestova TV (2008) Translation initiation on mammalian mRNAs with structured 5′UTRs requires DExH-box protein DHX29. *Cell* **135:** 1237–1250

Rajagopal V, Park EH, Hinnebusch AG, Lorsch JR (2012) Specific domains in yeast eIF4G strongly bias the RNA unwinding activity of the eIF4F complex towards duplexes with 5′-overhangs. *J Biol Chem* **287:** 20301–20312

Sagliocco FA, Vega Laso MR, Zhu D, Tuite MF, McCarthy JE, Brown AJ (1993) The influence of 5′-secondary structures upon ribosome binding to mRNA during translation in yeast. *J Biol Chem* **268:** 26522–26530

Sengoku T, Nureki O, Nakamura A, Kobayashi S, Yokoyama S (2006) Structural basis for RNA unwinding by the DEAD-box protein Drosophila Vasa. *Cell* **125:** 287–300

Shih JW, Tsai TY, Chao CH, Wu Lee YH (2008) Candidate tumor suppressor DDX3 RNA helicase specifically represses cap-dependent translation by acting as an eIF4E inhibitory protein. *Oncogene* **27:** 700–714

Shih JW, Wang WT, Tsai TY, Kuo CY, Li HK, Wu Lee YH (2011) Critical roles of RNA helicase DDX3 and its interactions with eIF4E/PABP1 in stress granule assembly and stress response. *Biochem J* **441:** 119–129

Soto-Rifo R, Limousin T, Rubilar PS, Ricci EP, Decimo D, Moncorge O, Trabaud MA, Andre P, Cimarelli A, Ohlmann T (2012) Different effects of the TAR structure on HIV-1 and HIV-2 genomic RNA translation. *Nucleic Acids Res* **40:** 2653–2667

Soto Rifo R, Ricci EP, Decimo D, Moncorge O, Ohlmann T (2007) Back to basics: the untreated rabbit reticulocyte lysate as a competitive system to recapitulate cap/poly(A) synergy and the selective advantage of IRES-driven translation. *Nucleic Acids Res* **35:** e121

Svitkin YV, Pause A, Haghighat A, Pyronnet S, Witherell G, Belsham GJ, Sonenberg N (2001) The requirement for eukaryotic initiation factor 4A (eIF4A) in translation is in direct proportion to the degree of mRNA 5′ secondary structure. *RNA* **7:** 382–394

Watts JM, Dang KK, Gorelick RJ, Leonard CW, Bess Jr. JW, Swanstrom R, Burch CL, Weeks KM (2009) Architecture and secondary structure of an entire HIV-1 RNA genome. *Nature* **460:** 711–716

Wilkinson KA, Gorelick RJ, Vasa SM, Guex N, Rein A, Mathews DH, Giddings MC, Weeks KM (2008) High-throughput SHAPE analysis reveals structures in HIV-1 genomic RNA strongly conserved across distinct biological states. *PLoS Biol* **6:** e96

Yang Q, Del Campo M, Lambowitz AM, Jankowsky E (2007) DEAD-box proteins unwind duplexes by local strand separation. *Mol Cell* **28:** 253–263

Yang Q, Jankowsky E (2006) The DEAD-box protein Ded1 unwinds RNA duplexes by a mode distinct from translocating helicases. *Nat Struct Mol Biol* **13:** 981–986

Yedavalli VS, Neuveut C, Chi YH, Kleiman L, Jeang KT (2004) Requirement of DDX3 DEAD box RNA helicase for HIV-1 Rev-RRE export function. *Cell* **119:** 381–392

 